EMBO
reports

MITRAC15/COA1 promotes mitochondrial translation in a ND2 ribosome–nascent chain complex

Cong Wang[1,2], Ricarda Richter-Dennerlein[1,2] (ID), David Pacheu-Grau[1], Fan Liu[3], Ying Zhu[3],
Sven Dennerlein[1] & Peter Rehling[1,2,4,*] (ID)

Abstract

The mitochondrial genome encodes for thirteen core subunits of the oxidative phosphorylation system. These proteins assemble with imported proteins in a modular manner into stoichiometric enzyme complexes. Assembly factors assist in these biogenesis processes by providing co-factors or stabilizing transient assembly stages. However, how expression of the mitochondrial-encoded subunits is regulated to match the availability of nuclear-encoded subunits is still unresolved. Here, we address the function of MITRAC15/COA1, a protein that participates in complex I biogenesis and complex IV biogenesis. Our analyses of a MITRAC15 knock-out mutant reveal that MITRAC15 is required for translation of the mitochondrial-encoded complex I subunit ND2. We find that MITRAC15 is a constituent of a ribosome–nascent chain complex during ND2 translation. Chemical crosslinking analyses demonstrate that binding of the ND2-specific assembly factor ACAD9 to the ND2 polypeptide occurs at the C-terminus and thus downstream of MITRAC15. Our analyses demonstrate that expression of the founder subunit ND2 of complex I undergoes regulation. Moreover, a ribosome–nascent chain complex with MITRAC15 is at the heart of this process.

Introduction

Mitochondria play key roles in energetic metabolism of eukaryotic cells by providing ATP generated by the oxidative phosphorylation system (OXPHOS). The oxidative phosphorylation system is composed of complexes I, II, III, and IV, which facilitate electron transport and translocation of protons across the inner mitochondrial membrane, and the ATP generating F_1F_o ATP synthase (complex V). Complexes I, III, IV, and V consist of subunits of dual genetic origin. While their 13 core proteins are mitochondrial-encoded and synthesized by membrane-bound mitochondrial ribosomes, the majority of the structural subunits are nuclear-encoded and imported from the cytosol [1–4]. Mitochondrial-encoded proteins are inserted into the inner membrane by the insertase OXA1L, which binds to mitochondrial ribosomes [3,5,6]. The fact that gene products, which are provided by two spatially separated translation systems, need to assemble in stoichiometric complexes necessitates coordination of the assembly processes.

To coordinate and regulate the assembly of the complexes of the oxidative phosphorylation system, a plethora of assembly factors are required. These assembly factors represent a functionally heterogeneous group of proteins that fulfill different and mostly complex-specific functions [7–10].

Although the molecular function and mode of action of assembly factors often remain elusive, they have been instrumental in defining maturation stages and regulatory processes in the biogenesis pathway. Many of these assembly factors have been linked to severe human disorders mostly affecting high-energy-demanding organs, such as heart, liver, muscle, or brain [11,12]. Due to the underlying block in the biogenesis process, an accumulation of assembly intermediates has frequently been observed in patients with mitochondrial disorders [11,13–15].

It is becoming increasingly clear that assembly of the oxidative phosphorylation system complexes occurs in a modular fashion [7]. In recent analyses, the biogenesis of the NADH:coenzyme Q oxidoreductase (complex I) was mapped in detail by defining assembly intermediates with mass spectrometric approaches [16,17]. Complex I assembly progresses through six distinct modules (membrane modules: ND1/P_P-a, ND2/P_P-b, ND4/P_D-a, ND5/P_D-b; matrix modules: N and Q), which preassemble to a certain degree, but are mostly metastable if assembly does not progress [16]. It is believed that the ND2/P_P-b module, which

1 Department of Cellular Biochemistry, University Medical Center Göttingen, Göttingen, Germany
2 Cluster of Excellence "Multiscale Bioimaging: from Molecular Machines to Networks of Excitable Cells" (MBExC), University of Goettingen, Goettingen, Germany
3 Leibniz-Forschungsinstitut for Molecular Pharmacology (FMP), Berlin, Germany
4 Max Planck Institute for Biophysical Chemistry, Göttingen, Germany
*Corresponding author. Tel: +49 551 395947; E-mail: peter.rehling@medizin.uni-goettingen.de

contains the mitochondrial-encoded ND2, represents the core module onto which the other modules assemble [16,17]. In case of cytochrome *c* oxidase (complex IV), three mitochondrial-encoded core components COX1, COX2, and COX3 assemble with imported structural subunits [9]. COX1 synthesis represents the starting point for complex IV assembly [18]. In human mitochondria, the assembly of COX1 occurs through an intermediate termed MITRAC complex (mitochondrial translation regulation assembly intermediate of cytochrome *c* oxidase) [18–20]. A lack of the MITRAC components MITRAC12 (COA3) or C12ORF62 (COX14) has been shown to affect COX1 translation. Therefore, these proteins represent translational regulators of COX1 [18,19,21,22]. These proteins are also at the heart of a control mechanism that adapts COX1 synthesis to cellular demands [18]. A stalled ribosome–nascent chain complex consisting of a partially synthesized and membrane integrated COX1 is associated with C12ORF62 and MITRAC12. Import of structural subunits relieves the elongation block and allows completion of COX1 synthesis. Whether similar translational control mechanisms also exist for other complexes remains unknown. For complex I, translational regulators have been suggested, but how they impact translation is unknown [23–26].

Here, we report on the function of MITRAC15 in complex I biogenesis. MITRAC15 participates in complex I biogenesis and IV biogenesis, preferentially interacting with the ND2/P_p-b module. Our analyses show that MITRAC15 is a specific translation regulation factor for ND2 and directly interacts with the mitochondrial ribosome during ND2 synthesis. MITRAC15 promotes the progression of ND2 assembly prior to ACAD9 association. While deletion of MITRAC15 reduces ND2 synthesis, the loss of ACAD9 prevents association of ND3 and ND4L with the ND2/P_p-b module. Hence, our study reveals MITRAC15 as translational regulator of the complex I subunit ND2 and demonstrates that transient ribosome–nascent chain complexes with specific ND2 translation intermediates are present at the start of the assembly process.

Results and Discussion

MITRAC15/COA1, a constituent of complex I and IV assembly intermediates

Respiratory chain complexes I, III, IV and V are built from mitochondrial- and nuclear-encoded subunits. The biogenesis of these complexes progresses through a series of distinct intermediates mediated by assembly factors. Assembly factors are proteins that assist at specific stages of the biogenesis process. The molecular functions of assembly factors are diverse, such as stabilizing transient folding states or providing co-factors. However, most assembly factors are specific to the assembly of one of the complexes. MITRAC15/COA1 was identified as a constituent of the COX1 assembly processes and has been shown to be associated with COX1 in the MITRAC assembly intermediate [19]. Recent analyses detected MITRAC15 present in two assembly processes; therefore, we immunoisolated the MITRAC assembly intermediate with MITRAC12 antibodies. As expected, MITRAC15 co-isolated with MITRAC12 and other MITRAC constituents (Fig 1A). However, compared to COX1 and C12ORF62, MITRAC15 was substantially less enriched in the eluate (Fig 1A). Accordingly, under our

experimental conditions a significant fraction of MITRAC15 appears to be not associated with MITRAC12. To define the MITRAC15-containing complexes, wild-type mitochondria were subjected to two-dimensional electrophoresis (2D PAGE, blue native PAGE followed by SDS–PAGE) and analyzed by Western blotting (Fig 1B). In contrast to MITRAC12, which was present in MITRAC complexes together with COX1, MITRAC15 mainly migrated in the low molecular weight range and in a complex of approximately 500 kDa. Interestingly, the 500 kDa MITRAC15 complex co-migrated with a complex formed by the complex I assembly factor ACAD9 (Fig 1B). Based on this finding, we concluded that in HEK293 cell mitochondria, only a minor fraction of MITRAC15 is present in the MITRAC complex. The larger fraction of MITRAC15 appears to be part of the early complex I assembly module ND2/P_p-b, which contains ACAD9 and MITRAC15 [17]. To further dissect MITRAC15-containing protein complexes, native immunoisolation analyses were carried out using mitochondria containing MITRAC12^{FLAG} or ACAD9^{FLAG}. Purified complexes were analyzed by 2D PAGE and Western blotting (Fig 1C). Upon isolation of MITRAC12^{FLAG}-containing complexes, we identified MITRAC15 together with COX1 and TIM21 in MITRAC complexes between 132 and 440 kDa. In contrast, MITRAC15 and ND2 were co-purified with ACAD9^{FLAG}, which migrated in larger complexes (440 and 880 kDa) and likely represents the ND2/P_p-b module (Fig 1C). Interestingly, MITRAC complexes were not co-isolated with ACAD9^{FLAG}, implicating that MITRAC15 is present in distinct complexes.

To exclude an involvement of MITRAC12 in the assembly of the ND2/P_p-b module and to support the idea of MITRAC15 acting in two distinct assembly pathways, a tandem immunoprecipitation experiment was performed. For this, MITRAC15^{FLAG}-containing complexes were first isolated via anti-FLAG immunoisolation. The purified fraction was subjected to a second isolation regime using an antibody against MITRAC12. MITRAC constituents, such as COX1 or COX4-1, and the ND2/P_p-b module components ACAD9 and ND2 were present in the first isolation step via MITRAC15^{FLAG}. However, ACAD9 and ND2 were absent from the eluate of the MITRAC12 immunoprecipitation (Fig 1D). Accordingly, MITRAC15 is present in the ND2/P_p-b module of complex I and in the MITRAC assembly intermediate of complex IV.

Functional segregation of MITRAC15 into assembly modules

To assess formation of MITRAC15-containing assembly modules with mitochondrial-encoded proteins, MITRAC15^{FLAG} was immunoisolated after radiolabelling of mitochondrial translation products. MITRAC15^{FLAG} co-purified predominantly ND2. Only small amounts of the complex I subunits ND3 and ND4L, and the complex IV constituents COX1 and COX2/3 were co-isolated with MITRAC15^{FLAG} (Fig 2A). In contrast, MITRAC12^{FLAG} preferentially co-purified COX1 and COX2 (see also Refs. [19,20]). Next, we purified MITRAC15^{FLAG}-containing complexes under native conditions and performed 2D-PAGE analyses. MITRAC15^{FLAG} isolated one complex that migrated between 132 and 440 kDa representing the co-purified MITRAC complex, as determined by the presence of MITRAC12. The second complex represented the ND2/P_p-b module (440–880 kDa) as indicated by the presence of ND2 and ACAD9. Interestingly, MITRAC15^{FLAG} also isolated TIM21, which only
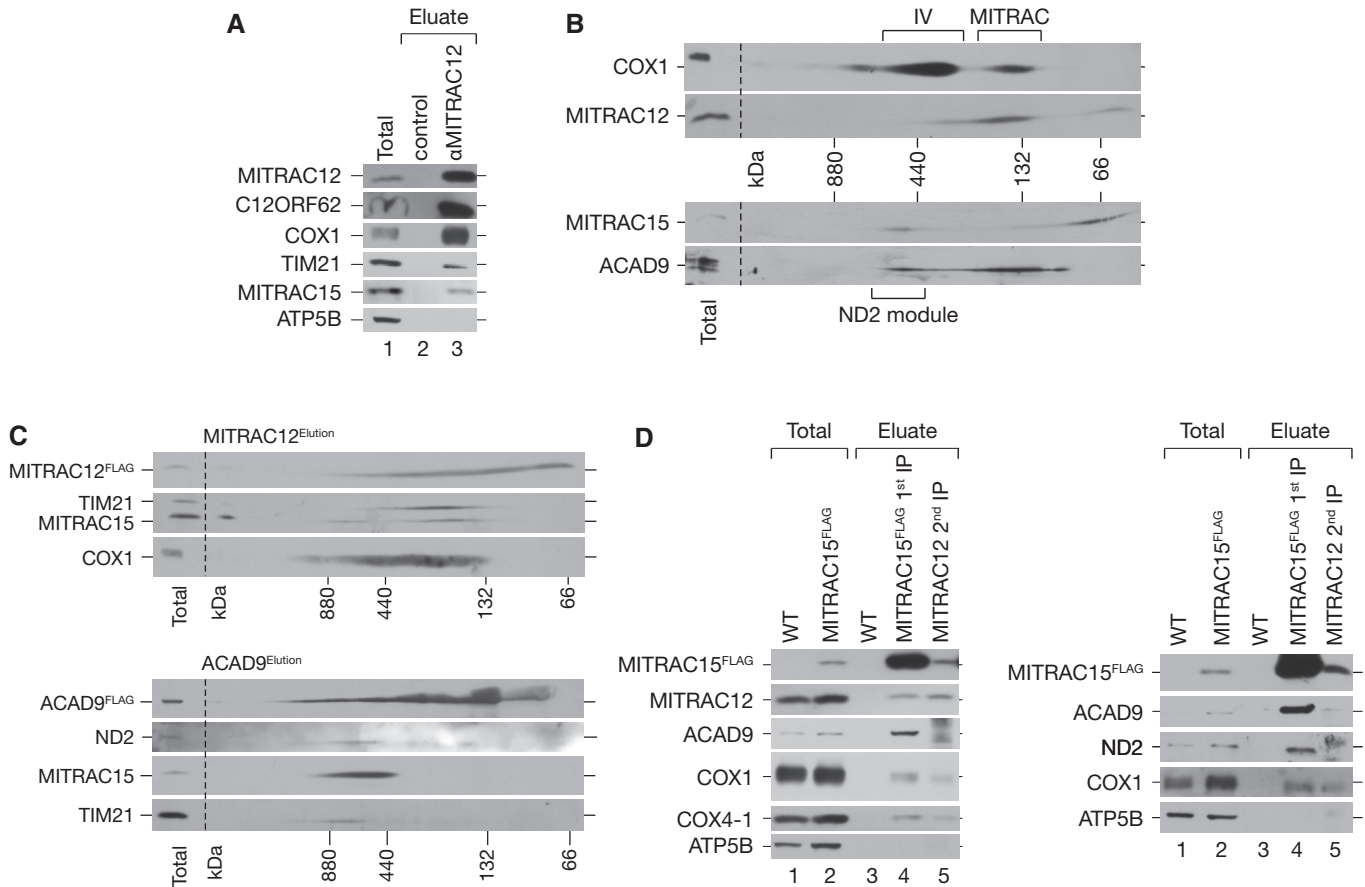
Figure 1. MITRAC15 interacts with distinct intermediates of complex I and complex IV.

A Solubilized mitochondria from wild-type HEK293T cells were subjected to immunoisolation with MITRAC12 antiserum. Eluates were analyzed by SDS–PAGE and Western blotting. Total 1.5%, eluate 100%.

B Wild-type mitochondria were solubilized and subjected to 2D-BN/SDS–PAGE and Western blotting with indicated antibodies.

C Solubilized mitochondria from MITRAC12^{FLAG}- or ACAD9^{FLAG}-expressing cells were subjected to anti-FLAG immunoisolation and native elution. Eluates were analyzed by 2D-BN/SDS–PAGE and Western blot analysis. Total 0.8% (MITRAC12^{FLAG} isolation), 0.35% (ACAD9^{FLAG} isolation), eluate 100%.

D Solubilized mitochondria from MITRAC15^{FLAG}-expressing cells were first subjected to native anti-FLAG immunoisolation (total 0.1%, eluate 10%, lane 4). Purified complexes were applied to anti-MITRAC12 immunoisolation (eluate 100%, lane 5). All samples were analyzed by SDS–PAGE and immunoblotting.

co-migrated with the ND2/P$_p$-b module but not with the MITRAC complex (Fig 2B). In the reverse experiment, TIM21^{FLAG} co-purified the MITRAC complex containing MITRAC12 and COX1. However, the co-isolated MITRAC15 was exclusively present in the ND2/P$_p$-b module together with ACAD9 (Fig 2B). We concluded that MITRAC15 and TIM21 are not jointly associated with the MITRAC complex; however, they are both present in the ND2/P$_p$-b module (Fig 2B).

The observation that MITRAC15 effectively co-purified ND2 but to a much lesser extent ND3 and ND4L suggested that it primarily associated early with ND2 and potentially even co-translationally (see also Fig 4B). When MITRAC15^{FLAG} was immunoisolated from mitochondria, MITRAC constituents (COX1, COX4-1, MITRAC12) and subunits of the ND2/P$_p$-b module (ND2, ACAD9) were co-purified (Fig 2C). In addition, we identified components of the mitochondrial ribosomal large (uL1m) and the small (mS40) subunits and the insertase OXA1L as MITRAC15-associated proteins. For comparison, we purified C12ORF62, which efficiently co-isolated

ribosomes, MITRAC constituents, but not ACAD9 or ND2. In contrast, an immunoisolation of ACAD9^{FLAG} did not co-purify the MITRAC component MITRAC12 but recovered MITRAC15 and TIM21 (Fig 2D). Accordingly, MITRAC15 and TIM21 are present in distinct complexes, one catering to COX1 biogenesis and the other linked to ND2. These observations are in agreement with a function of MITRAC15 during the ND2 translation process similar to C12ORF62 during COX1 synthesis [18].

MITRAC15 promotes ND2 translation

To assess the function of MITRAC15 in ND2 assembly, we used CRISPR/Cas9 technology to generate a MITRAC15 knockout (MITRAC15$^{-/-}$) cell line, in which both alleles contained a stop codon in exon 2 (Fig 3A). MITRAC15 knockout was verified by sequencing of the genomic locus and Western blot analyses (Fig 3B). Although MITRAC15 knockdown in fibroblasts affected the assembly pathway of complexes I and IV [19], in MITRAC15$^{-/-}$
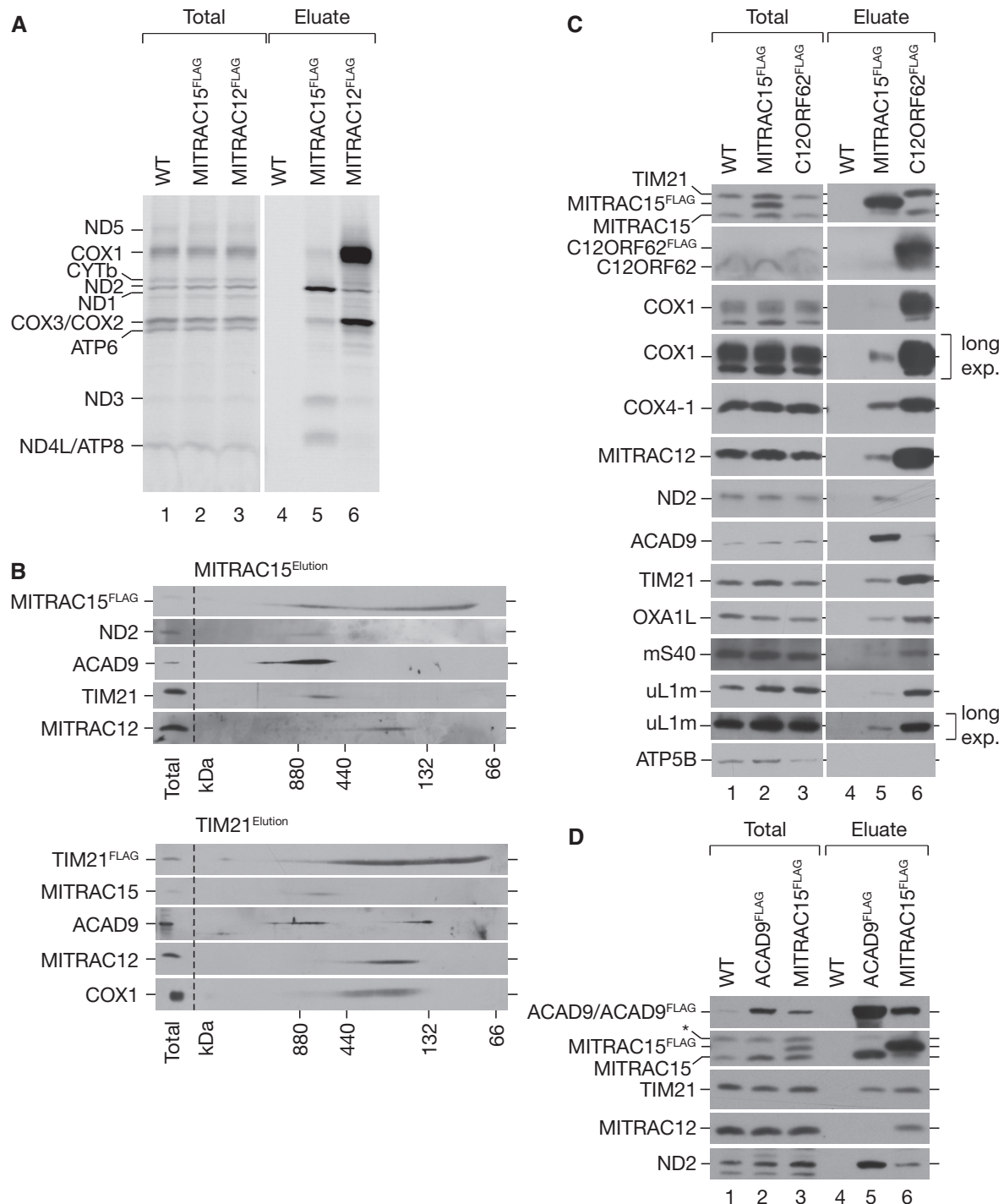
Figure 2. MITRAC15 interacts with mitochondrial ribosomes and isolates preferentially ND2.

A Mitochondrial translational products were labeled with [^{35}S]methionine, and anti-FLAG immunoisolation was performed as described in Fig 1D. Eluates were analyzed by SDS–PAGE and digital autoradiography. Total 1.5%, eluate 100 %.

B Solubilized mitochondria from MITRAC15^{FLAG}- or TIM21^{FLAG}-expressing cells were subjected to anti-FLAG immunoisolation and analyzed by 2D-BN/SDS–PAGE and Western blotting. MITRAC15^{FLAG} isolation: total 0.1%, eluate 100%. TIM21^{FLAG} isolation: total 0.2%, eluate 66% (TIM21^{FLAG} decoration), 33% (MITRAC15, ACAD9, MITRAC12, COX1 decoration).

C Solubilized mitochondria from MITRAC15^{FLAG}- or C12ORF62^{FLAG}- expressing cells were subjected to anti-FLAG immunoisolation and analyzed by SDS–PAGE and immunoblotting. Total 0.4%, eluate 100% (MITRAC15^{FLAG} isolation), 70% (C12ORF62^{FLAG} isolation).

D Solubilized mitochondria from ACAD9^{FLAG}- or MITRAC15^{FLAG}- expressing cells were subjected to anti-FLAG immunoisolation and analyzed by SDS–PAGE and immunoblotting. Total 0.5% (ACAD9^{FLAG} isolation), 0.4% (MITRAC15^{FLAG} isolation), eluate 100%. Asterisk (*) indicates TIM21 signal. ACAD9/ACAD9^{FLAG} could not be separated with the used gel system, both proteins are detected with ACAD9 antiserum.

HEK293T cells a decrease in ND2 and some of the tested nuclear-encoded complex I subunits was apparent, while other proteins remained unaffected. In agreement with this, when respiratory chain complexes were analyzed by BN-PAGE, loss of MITRAC15 leads to reduced levels of complex I by 40% (Fig 3C). For NDUFB10, faster migrating subcomplexes could be detected in MITRAC15$^{-/-}$ mitochondria, which likely represent assembly intermediates. This finding agrees with previous analyses that NDUFB10 assembles in a module independent from ND2 [16]. Moreover, we measure complex I activity in wild-type and MITRAC15$^{-/-}$ cells. Complex I activity was significantly reduced in MITRAC15$^{-/-}$ cells (Fig 3D, left bar graph), while citrate synthase activity was not affected (Fig 3D right bar graph). The observation that loss of MITRAC15 in HEK293T did not cause a reduction in complex IV contrasted with what we found in fibroblasts in which complexes I and IV were affected [19]. Apparently, the loss of MITRAC15 leads to different effects in different cell types and it is conceivable that MITRAC15 may carry out cell type-specific functions.

The observed reduction in complex I (Fig 3C and D), a preferential interaction of MITRAC15 with newly synthetized ND2 (Fig 2A), and the interaction between MITRAC15 and mitochondrial ribosomes (Fig 2C) led us to investigate whether the reduced level of ND2 could be attributed to a reduced *de novo* ND2 synthesis or an increased turnover. Thus, to investigate ND2 translation and stability in MITRAC15$^{-/-}$ cells, we performed pulse and pulse-chase [^{35}S] methionine labeling experiments (Fig 3E). Loss of MITRAC15 led to reduced ND2 synthesis by 40%, which matches the reduced levels of complex I (Fig 3E, lanes 1 and 3; left bar graph), while ND2 turnover was only marginally affected (Fig 3E, lanes 2 and 4; right bar graph). Expression of MITRAC15^{FLAG} in the MITRAC15$^{-/-}$ cells restored expression of ND2, demonstrating that the observed effects on ND2 translation are directly linked to MITRAC15 function (Fig 3F). Therefore, we concluded that the reduced abundance and activity of complex I in MITRAC15$^{-/-}$ cells resulted from a reduced synthesis of ND2 and hence a reduction of the ND2/P$_p$-b module.

MITRAC15 interacts with ND2 co-translationally

ACAD9 is a crucial factor for assembly of complex I. Patients carrying an ACAD9 mutation display a severe decrease in complex I and of the Q module subunit NDUFS3 [27]. Since ACAD9 was suggested to be present in the ND2/P$_p$-b together with MITRAC15 [17], we analyzed whether ACAD9 participated in the translation of ND2. To this end, we monitored the synthesis and stability of mitochondrial-encoded proteins by [^{35}S]methionine pulse and pulse-chase labeling in wild-type and MITRAC15$^{-/-}$ cells after reducing ACAD9 protein levels by siRNA treatments (Fig 4A). In wild-type cells, loss of ACAD9 led to a clear reduction in ND2 synthesis (approx. 54%). The depletion of ACAD9 in MITRAC15$^{-/-}$ cells did not exacerbate the reduction of ND2 translation compared to wild-type cells (Fig 4A, left graph). In chase analyses, the loss of ACAD9 led to a severe decrease in ND2 by about 90% in wild-type and MITRAC15$^{-/-}$ cells, which is indicative of an increased turnover of the protein (Fig 4A, right graph). Accordingly, loss of ACAD9 affected translation and stability of ND2. However, an additive effect of loss of MITRAC15 and loss of ACAD9 could not be observed, indicating that MITRAC15 and ACAD9 act in a sequential manner during ND2 translation. The observation that only ACAD9 and not

MITRAC15 was important for ND2 stability suggested to us that ACAD9 likely acts downstream of MITRAC15 and thus is critical for stabilizing ND2 during assembly of complex I, while MITRAC15 primarily acts as a translational regulator for ND2.

To define the epistasis of ACAD9 and MITRAC15 function, we assessed the interaction of MITRAC15 with newly synthesized mitochondrial-encoded proteins in the context of siRNA-mediated depletion of ACAD9 (Fig 4B). The interactions between MITRAC15^{FLAG} and newly synthesized COX1, COX2, and ND2 were not affected by the loss of ACAD9. In contrast, the interactions between MITRAC15 and the newly synthesized ND3 and ND4L were drastically reduced upon ACAD9 knockdown (Fig 4B). Hence, ACAD9 is not required for the MITRAC15/ND2 interaction but critical for integrating MITRAC15 into the ND2/P$_p$-b module, which contains ND3 and ND4L. We conclude that ACAD9 acts downstream of MITRAC15 during assembly of the ND2/P$_p$-b module.

C12ORF62 is an established translational activator for mitochondrial-encoded COX1 [18,19,22]. It is found in a complex with nascent COX1 polypeptide chains and the mitochondrial ribosome but does not affect COX1 stability [18]. Similar to C12ORF62, MITRAC15 interacts with the mitochondrial ribosome and affects synthesis but not stability of a mitochondrial-encoded protein, ND2. Hence, we analyzed whether MITRAC15 interacted with ND2 nascent chains similar to C12ORF62 and COX1. To this end, we carried out [^{35}S]methionine labeling of mitochondrial translation products in the presence or absence of puromycin, which causes release of nascent chains from the ribosome. Subsequently, we assessed the interaction between MITRAC15 and newly synthesized ND2 (Fig 4C). MITRAC15^{FLAG} co-purified two distinct polypeptide chains in the presence of puromycin. Importantly, the fragments isolated by MITRAC15^{FLAG} did not resemble the COX1 fragments purified by C12ORF62^{FLAG} (Fig 4C). Furthermore, after puromycin treatment, we detected very small fragments that migrated faster than ND4L (Fig 4C, lanes 10 and 12). These fragments could be very small fragments of either ND2 or ND4L. Considering that MITRAC15 affects ND2 translation and is present in the ND2/P$_p$-b module, these analyses were in agreement with the idea that MITRAC15 is associated with a ND2 ribosome–nascent chain complex. To substantiate this conclusion and assess whether the ND2 fragments represented productive translation intermediates, we radiolabeled mitochondrial translation products with [^{35}S]methionine followed by a chase. Puromycin was added at different chase times to release ND2 nascent chains (Fig 4D). Already after 5 min of chase, ND2 nascent chains were no longer associated with MITRAC15^{FLAG}, while the amount of newly synthesized ND2 bound to MITRAC15 drastically increased by 36% (Fig 4D). Accordingly, ND2 nascent chains that are associated with MITRAC15 represent productive intermediates that eventually mature into full-length ND2. In summary, MITRAC15 can be described as a translation-affecting factor for ND2 that is associated with the mitochondrial ribosome during ND2 synthesis.

ACAD9 binds to the C-terminal portion of ND2

The loss of ACAD9 affected ND2 translation and stability (Fig 4A). Based on the observed association between MITRAC15 and ND2 nascent chains, we analyzed whether ACAD9 similarly associated with translation intermediates of ND2 (Fig 5A). However, in
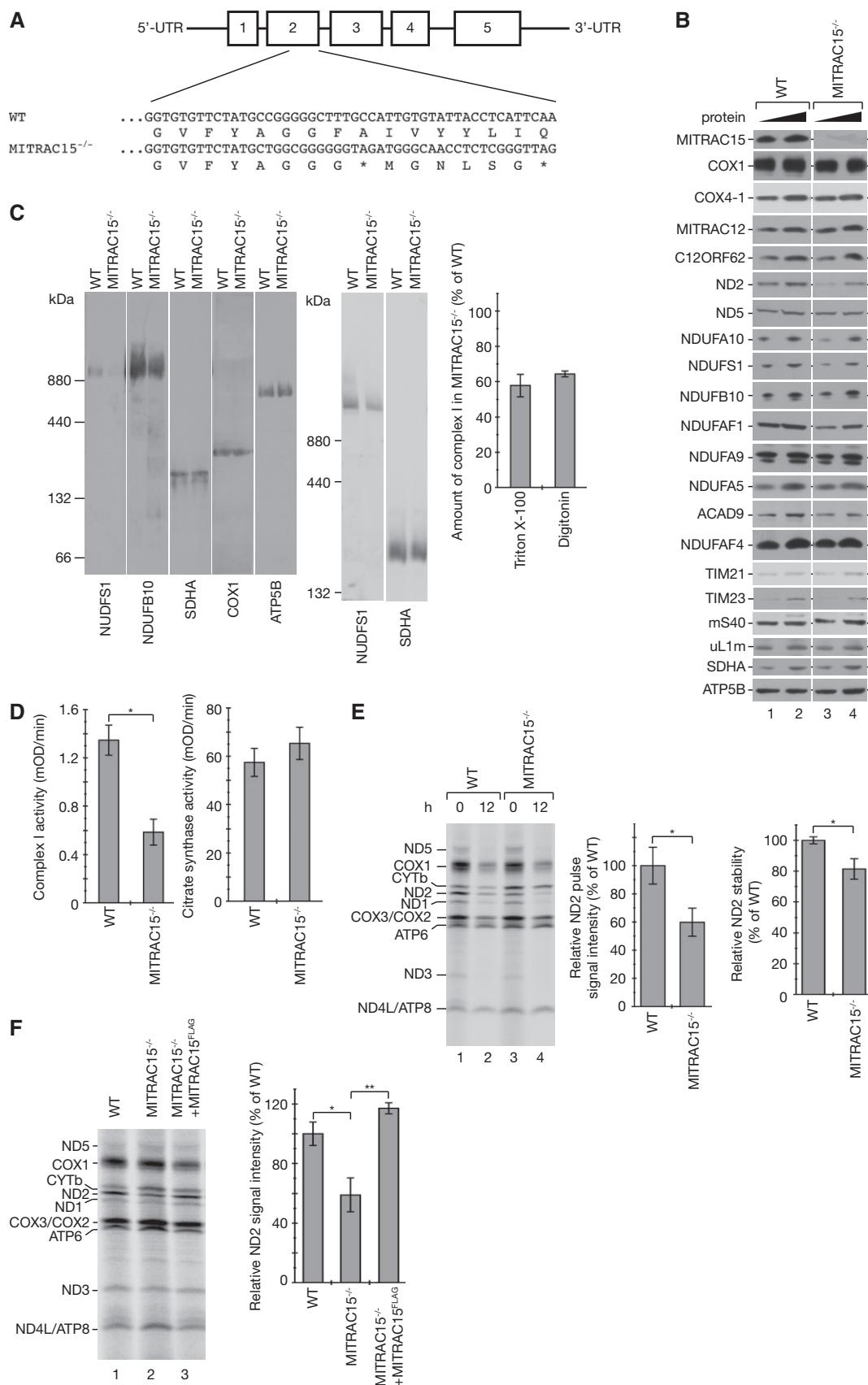
Figure 3.

Figure 3.   MITRAC15 affects ND2 translation.

A   A knockout cell line of MITRAC15 (MITRAC15$^{-/-}$) was created in HEK293T cells by using CRISPR/Cas9 technology. Alignment of respective mutated region compared to wild type shows premature STOP codons (*) in MITRAC15$^{-/-}$.

B   Mitochondria from wild-type and MITRAC15$^{-/-}$ cells were isolated and subjected to steady-state protein analyses by Western blotting.

C   Mitochondria from wild-type and MITRAC15$^{-/-}$ cells were isolated and analyzed by BN-PAGE. Triton X-100 (left site) or digitonin (right site) was used for solubilization. The amount of complex I was quantified utilizing the NDUFS1 signal and normalized against SDHA levels (error bars indicate SEM from three biological replicates).

D   Complex I and citrate synthase activity were measured in WT and MITRAC15$^{-/-}$ cells (error bars indicate SEM from three biological replicates; *$P < 0.05$; unpaired t-test).

E   Pulse-chase [^{35}S]methionine radiolabeling of mitochondrial translation products in wild-type and MITRAC15$^{-/-}$ cells. Samples were analyzed by SDS–PAGE and digital autoradiography. Signal intensity of ND2 was normalized to the ATP6 signal, and the relative ND2 stability was calculated by relative chase ND2 signal/relative pulse ND2 signal (error bars indicate SEM from three biological replicates; *$P < 0.05$; unpaired t-test).

F   Pulse radiolabeling after re-expressing MITRAC15^{FLAG} in MITRAC15$^{-/-}$ cells. Samples were analyzed by SDS–PAGE and digital autoradiography. Relative pulse signal intensity of ND2 was normalized to ATP6 (error bars indicate SEM from three biological replicates; *$P < 0.05$; **$P < 0.01$; unpaired t-test).

contrast to MITRAC15, nascent chains of ND2 did not co-purify with ACAD9. We therefore concluded that ACAD9 is not present during ND2 translation.

To analyze whether ACAD9 was required for the interaction between MITRAC15 and ND2 nascent chains, we depleted ACAD9 by siRNA treatment. Considering that ACAD9 depletion reduces ND2 translation (Fig 4A), the interaction between MITRAC15 and ND2 nascent chains remained unaffected (Fig 5B). Thus, ACAD9 does not interact with ND2 translation intermediates and does not influence the interaction of MITRAC15 with the nascent or mature ND2, which was in agreement with the idea that ACAD9 joins the ND2/P$_p$-b module downstream of MITRAC15.

An explanation for the lack of interaction between ACAD9 and ND2 nascent chains could be that ACAD9 binds only to the full-length ND2 polypeptide. In an initially unrelated analysis, we investigated interaction sites between mouse mitochondrial proteins using chemical crosslinking in combination with mass spectrometric analyses. These analyses identified a single crosslink between ACAD9 and a matrix-facing peptide loop at the C-terminus of ND2 (Fig 5C). The crosslinked peptide identified for ACAD9 consisted of 23 amino acids, and most of this sequence, as well as the crosslinked Lys^{504}, is conserved between human being and mouse. For ND2, a peptide with the size of 7 amino acids was identified and a short "TK motif" next to the crosslinked Lys^{319} is conserved between human being and mouse, but not the Lys^{319} itself. This crosslink indicates that ACAD9 interacts with ND2 when the C-terminal portion has been synthesized, in line with our conclusions on the functional order of ACAD9 and MITRAC15 in the assembly process.

Conclusion

In this study, MITRAC15 could be identified in distinct complexes of complex IV (MITRAC) and complex I (ND2/P$_p$-b module) assembly line. Based on in silico data, MITRAC15 has been suggested to represent a homologue of the S. cerevisiae COA1, a protein that participates in complex IV biogenesis [3,4,9]. However, S. cerevisiae lacks complex I and COA1 has not been analyzed in other yeast species that possess complex I. Hence, it is open if a role of MITRAC15/COA1 in complex I biogenesis was acquired during evolution. MITRAC15 represents the first complex I translation factor, which interacts with a mitochondrial-encoded subunit (ND2) during translation, while having little effect on its stability. ACAD9 acts downstream of MITRAC15 in the assembly of the ND2/P$_p$-b module and as a major player for the incorporation of the mitochondrial-encoded subunits ND3 and ND4L into the ND2/P$_p$-b module, while it is not present during ND2 translation. However, ACAD9 was shown to be important for both synthesis and stability of mitochondrial ND2. Since ACAD9 is not present during translation of ND2, the question remains how it is able to influence this process. A possible answer involves the complex I assembly factor NDUFAF1. Dunning et al [26] reported that a patient mutation in NDUFAF1 was able to cause a severe decrease in ND2 upon radiolabeling of mitochondrial-encoded proteins [26]. Considering that a decrease in ACAD9 protein levels causes a lower abundance of NDUFAF1 [27], the effect of ACAD9 on ND2 translation could likely be caused indirectly through NDUFAF1. Whether MITRAC15 directly affects translation or whether it acts in an indirect manner will require further analyses.

Figure 4.   MITRAC15 interacts with nascent chains of ND2.

A   Mitochondrial translation products were radiolabeled with [^{35}S]methionine after siRNA-mediated depletion of ACAD9 in wild-type and MITRAC15$^{-/-}$ cells. Cell lysates were analyzed by SDS–PAGE and digital autoradiography. For quantifications, the signal intensity of ND2 was normalized to ATP6 and the relative ND2 stability was calculated by relative chase ND2 signal/relative pulse ND2 signal (error bars indicate SEM from three biological replicates; *$P < 0.05$; **$P < 0.01$; ***$P < 0.001$; unpaired t-test).

B   FLAG immunoprecipitation was performed in mitochondrial extracts from MITRAC15^{FLAG}-expressing cells after siRNA-mediated downregulation of ACAD9 and pulse radiolabeling. SDS–PAGE followed by autoradiography was used to analyze eluates. Relative signal intensity of ND2, ND3, and ND4L was normalized to ATP6 (total) or isolation efficiency (eluate). Total 2%, eluate 100%. Error bars indicate SEM from three biological replicates; **$P < 0.01$; unpaired t-test.

C   After C12orf62 downregulation, [^{35}S]methionine labeling was performed. During labeling, mitochondrial translation was inhibited with puromycin (pur) (2 μg/ml). MITRAC15^{FLAG}-interacting nascent chains were isolated by FLAG immunoprecipitation from cell lysates. Eluates were subjected to SDS–PAGE and analyzed by digital autoradiography. Total 2%, MITRAC15^{FLAG} eluate 100% (in case of C12ORF62^{FLAG}, 25% of eluate was loaded as a standard). Red asterisks, accumulating nascent chains of ND2. The accumulating nascent chains of ND2 of lane 12 are presented in a magnification. F1-F3 mark nascent chains of COX1 [18].

D   HEK293T cells were pulse-labeled with [^{35}S]methionine in the presence of puromycin (2 μg/ml). During puromycin treatment, cells were incubated for 5 and 10 min in medium lacking [^{35}S]methionine. Anti-FLAG immunoisolations were performed as described and eluates analyzed as described in (C). Total 1%, eluate 100%. The signal of ND2 was graphed after normalization against the COX2 signal, and the signal of mature ND2 in the 5-min chase sample was set as 100% (error bars indicate SEM from three biological replicates; *$P < 0.05$; paired t-test). Red asterisks, accumulating nascent chains of ND2.
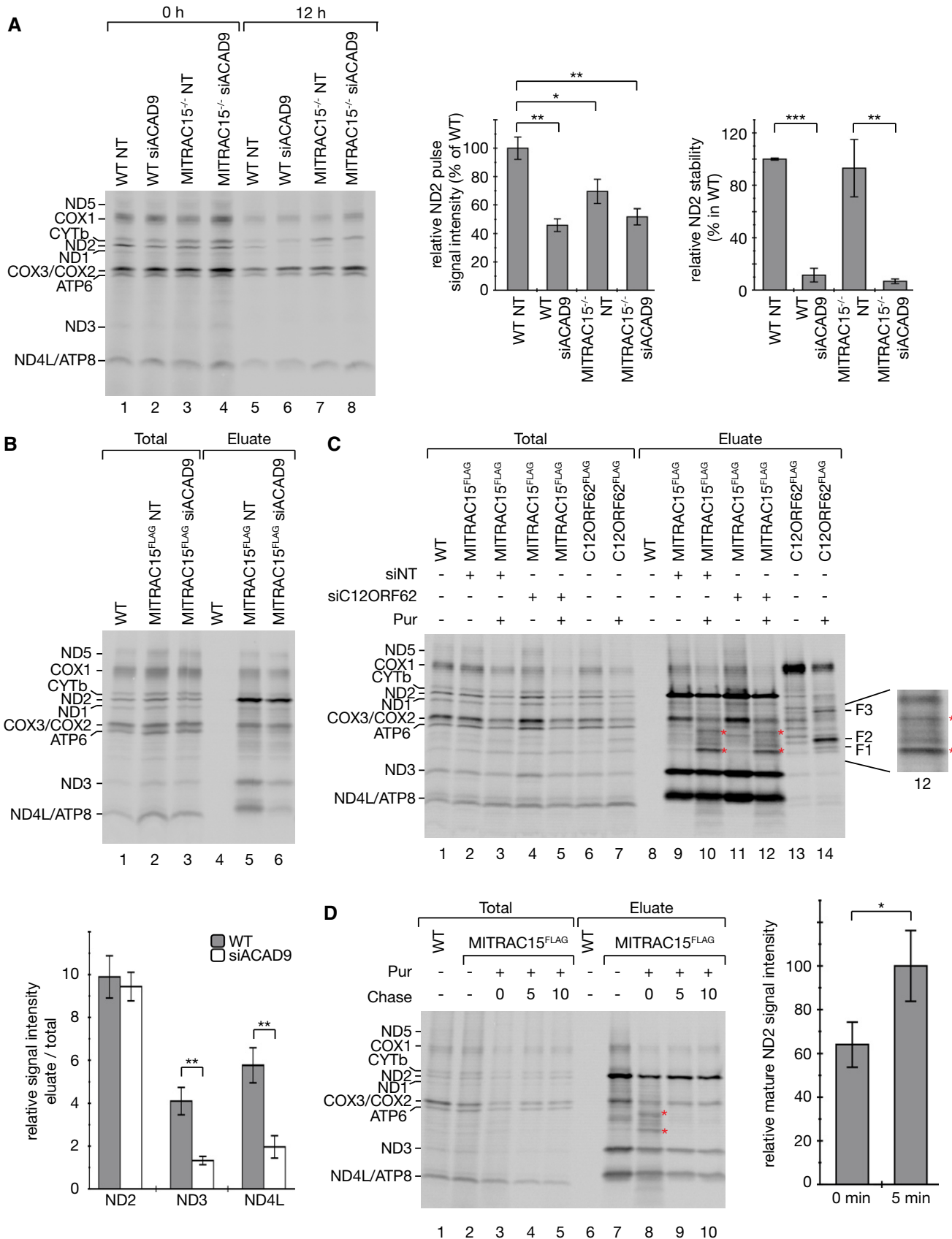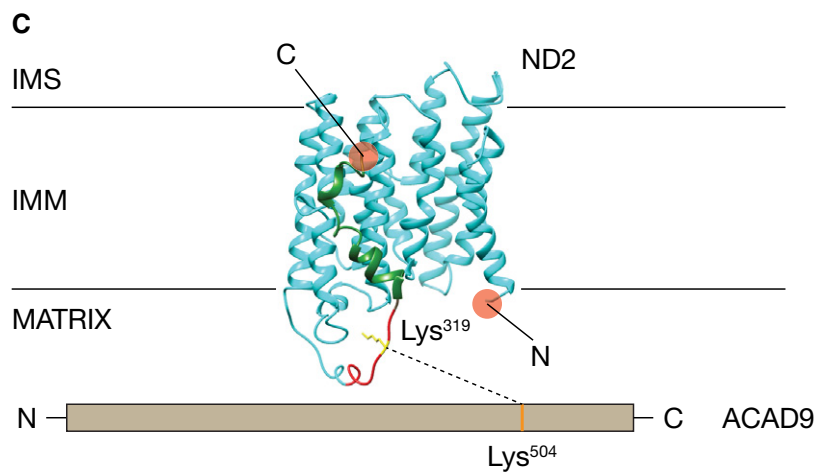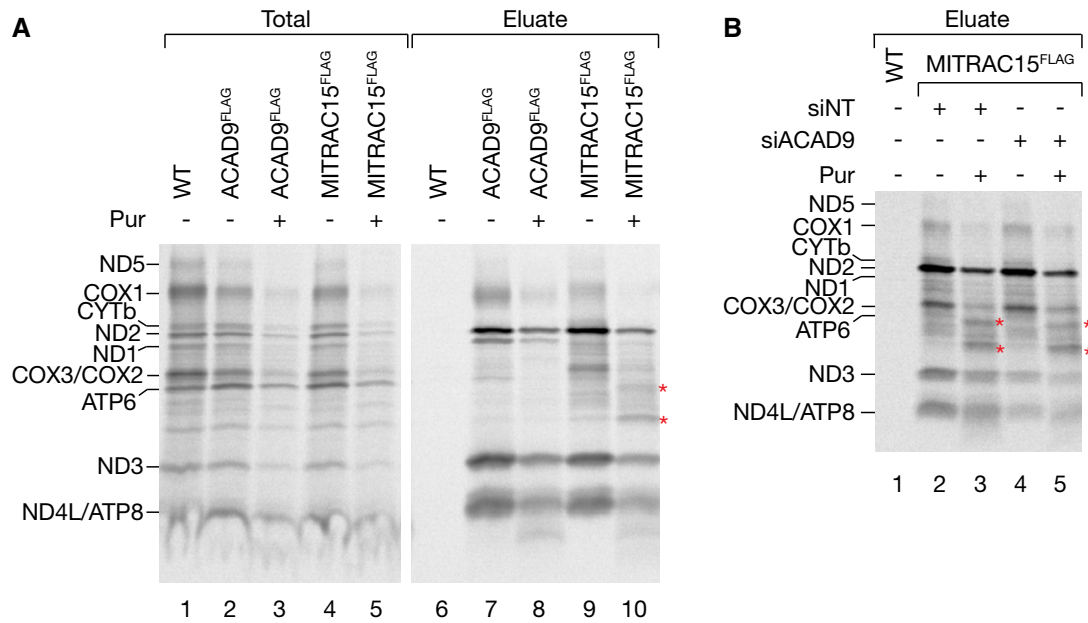
Figure 4.

Figure 5. ACAD9 is not present during ND2 translation.

A, B Radiolabeling with [35S]methionine, anti-FLAG immunoisolation, and sample analyses were performed as described in Fig 4C. (B) Depletion of ACAD9 by siRNA was performed as in Fig 4A. Total 1%, eluate 100%. Red asterisks, accumulating nascent chains of ND2.

C Identified crosslink between murine ACAD9 and ND2 (spectrum in Fig EV1). ND2: red—crosslinked peptide, green—C-terminal helix, yellow—crosslinked Lys319. ACAD9: orange—crosslinked Lys504. Sequences of identified crosslinked peptides from mouse and the homologous sequences from the human proteins are presented (yellow: crosslinked lysine).

Materials and Methods

Cultivation of human cells

The HEK293-Flp-In™ T-REx™ (HEK239T) (Thermo Fisher) cell lines were cultured in high glucose DMEM, supplemented with 10% (v/v) FBS (Biochrom), 2 mM L-glutamine, 1 mM sodium pyruvate, and 50 μg/ml uridine, under a 5% CO_2 humidified atmosphere at 37°C. Cells were passaged upon reaching confluence. Cell lines were regularly tested for mycoplasma contamination.

Generation of stable cell lines

Cell lines expressing ACAD9[FLAG] under the control of a tetracycline-inducible promoter were generated in HEK293T cells as described previously [19]. Briefly, HEK293T wild-type cells were transfected with the pcDNA5/FRT/TO vector containing the sequence of ACAD9[FLAG] and the pOG44 vector using GeneJuice (Novagen) as transfection reagent. Selection of transfected cells was performed with Hygromycin (100 μg/ml), and single-cell colonies were selected for analysis with SDS–PAGE followed by immunoblotting. The MITRAC12[FLAG], MITRAC15[FLAG] TIM21[FLAG], and C12ORF62[FLAG] cell lines were generated in previous studies in our laboratory [18,19].

Generation of knockout cell lines

The generation of knockout cell lines by the CRISPR/Cas9 system was performed as previously described by Ran *et al* [28]. Guide selection was performed with software provided by the laboratory of Prof. Feng Zhang [29]. The selected guide was cloned into the pX330 vector using the primers: 5′-CACCGATTATCTCAAGCTCAT CGACAGG-3′ (forward) and 5′-AAACCCTGTCGATGAGCTTGAGAT AATC-3′ (reverse). HEK239T cells were transfected with pX330 vector together with an EGFP-containing plasmid (pEGFP-N1; Clontech Laboratories, Inc). Single cells were sorted using a FACS Vantage SE machine and the knockouts confirmed by SDS–PAGE and Western blotting. To determine the exact mutation, sequencing of the MITRAC15 genomic locus was performed (forward primer: 5′-T TTGCTGGGCTTCTTATGCATATTAG-3′, reverse primer: 5′-TTCAAA ATATGAAAGGAGCCAGTGAC-3′).

siRNA-mediated depletion experiments

To downregulate protein of interest in HEK239T cells, the following siRNA oligonucleotides were used for transfection (sense strand is given): ACAD9: 5′-GGUCGUUGAUUCUGAUGGA-3′, C12ORF62: 5′-CA GUCCUGUUCACAAAGAA-3′, non-targeting control siRNA (Eurogentec). Lipofectamine RNAi-MAX (Invitrogen) was used as transfection reagent, following the manufacturer's instructions. After the transfection, cells were cultured for 72 h as described above.

Isolation of mitochondria

Protocols for isolating human mitochondria were modified according to Ref. [19]. Cells were harvested, washed with PBS, and resuspended in TH buffer (300 mM Trehalose 10 mM KCl, 10 mM HEPES, pH 7.4) with 0.1 mg BSA/ml. Cells were homogenized twice using a Potter S dounce homogenizer (Sartorius) and pelleted

at 400× *g*, 10 min at 4°C after each homogenization step. The supernatant was collected and remaining debris removed by centrifugation (7 min, 4°C, 800× *g*). The supernatant was collected and mitochondria pelleted by centrifugation at 11,000× *g* for 10 min at 4°C. BSA was removed by washing the mitochondria with BSA-free TH buffer collected by centrifugation as before for 5 min. For protein determination, the mitochondrial pellet was suspended in BSA-free TH buffer or stored at −80°C until use.

Immunoisolation of protein complexes

Isolated mitochondria or cells were solubilized in lysis buffer (150 mM NaCl, 10% glycerol (v/v), 20 mM $MgCl_2$, 1 mM PMSF, 50 mM Tris–HCl, pH 7.4, with 1% digitonin (v/w)) at a protein concentration of 1–2 μg/μl for 30 min at 4°C and 1,000 rpm. Lysates were cleared by a 15-min centrifugation step at 4°C and 20,000× *g*. The supernatant was then transferred onto anti-FLAG M2 agarose beads (Sigma-Aldrich) for FLAG immunoprecipitation or onto protein A-Sepharose (PAS) containing crosslinked MITRAC12 antibody in a Mobicol spin column (MoBiTec). After 1-h incubation on an end-over-end shaker at 4°C, the unbound proteins were removed by spinning out the supernatant for 1 min, 200× *g* at 4°C. The beads were washed ten times with washing buffer (150 mM NaCl, 10% glycerol (v/v), 20 mM $MgCl_2$, 1 mM PMSF, 50 mM Tris–HCl, pH 7.4, with 0.1% digitonin (v/w)). For FLAG immunoprecipitation, elution was performed with washing buffer containing 0.4 mg/ml FLAG peptide (Sigma) for 30 min at 1,000 rpm, 4°C. Bound proteins at PAS-αMITRAC12 columns were eluted for 5 min by adding 0.1 M glycine, pH 2.8, and 750 rpm shaking at room temperature.

[35S]methionine labeling of newly synthesized mitochondrial-encoded proteins

For pulse labeling of newly synthesized mitochondrial proteins, cells were starved with FCS/methionine-free DMEM. During the [35S]methionine incorporation, the media were replaced with fully supplemented DMEM lacking methionine. Cytosolic translation was inactivated by emetine for pulse labeling or anisomycin for pulse-chase analysis, and 0.2 mCi/ml [35S]methionine was added. After 1-h incubation, cells were either harvested with PBS (pulse labeling) or the radiolabeling media were exchanged with fully supplemented DMEM and cells were further grown for 12 h (chase) before harvesting with PBS. Samples were further analyzed by SDS–PAGE and autoradiography. Signals were detected on Storage Phosphor Screens with a Typhoon FLA 7000 scanner (GE Healthcare). For quantifications, ImageQuant TL software (GE Healthcare) was used. Puromycin-treated samples were pulse-labeled for 10 min before puromycin (2 μg/ml) addition and further incubated for 20 min.

Blue native/2D-SDS–PAGE analysis

BN-PAGE was performed as described previously [19]. Isolated mitochondria or cells were solubilized in BN-PAGE lysis buffer (20 mM Tris–HCl, 60 mM NaCl, 10% glycerol (v/v), 1 mM EDTA, 1 mM PMSF with 1% digitonin or 1% Triton X-100 (v/w)) with a protein concentration of 1 μg/μl. The lysate was incubated for 20 min on ice and debris removed by 15-min centrifugation at 4°C and 20,000× *g*. BN-PAGE sample buffer (5% Coomassie Brilliant

Blue G-250 (v/w), 500 mM 6-aminocaproic acid, 100 mM Bis-Tris–HCl, pH 7.0) was added to the supernatant, and the sample was subjected to electrophoresis on a 4–13% gradient gel as described by Wittig *et al* [30]. After electrophoresis, proteins were either transferred onto PVDF membranes or further subjected to 2D-PAGE analysis. For 2D PAGE, the BN-PAGE lane of interest was cut out and subjected to a second-dimension SDS–PAGE separation.

Enzymatic assays

The activity of mitochondrial complex I was assessed by the ab109721 Complex I Enzyme Activity Assay Kit (Colorimetric). The measurements were carried out as described in the manual. The measurement was performed in a Synergy H1 Hybrid Multi-Mode Reader (BioTek). The enzymatic activity of Citrate synthase, a matrix protein encoded in the nDNA, was assayed following previously described protocols [31] and using a Synergy H1 Hybrid Multi-Mode Reader (BioTek).

Miscellaneous

After SDS–PAGE separation, proteins were transferred onto PVDF membranes (Millipore) by semidry blotting. Primary commercial antibodies used were as follows: ACAD9 (15770-1-AP, Proteintech, rabbit), ND2 (19704-1-AP, Proteintech, rabbit), mS40 (16139-1-AP, Proteintech, rabbit), NDUFB10 (ab196019, Abcam, rabbit), ND5 (55410-1-AP, Proteintech, rabbit), NDUFS1 (12444-1-AP, Proteintech, rabbit), NDUFAF4 (26003-1-AP, Proteintech, rabbit), NDUFA5 (16640-1-AP, Proteintech, rabbit), and NDUFB10 (ab192245, Abcam, rabbit). Home-made antibodies (MITRAC15, COX1, COX4-1, MITRAC12, C12ORF62, uL1 m, OXA1L, TIM21, TIM23, SHDA, ATP5B, NDUFA10, NDUFFAF1, and NDUFA9) were raised in rabbit. Membranes were probed with a secondary anti-rabbit antibody coupled to HRP, and signals were developed on X-ray films using the enhanced chemiluminescence detection kit (GE Healthcare).

Mitochondria purification and crosslinking

Mitochondria were purified from mouse heart (two C57BL/6N mice, 6–10 weeks old) using standard differential centrifugation methods. In brief, the heart was removed from the animal, pooled, and homogenized in a dounce homogenizer on ice (20 times, 1,000 rpm) in homogenization buffer (220 mM mannitol, 70 mM sucrose, 5 mM HEPES-KOH, pH 7.4, 1 mM EGTA-KOH, pH 7.4, 1 mM PMSF, 1 x Complete Protease Inhibitor EDTA-free). The homogenate was centrifuged at 800× *g* for 5 min at 4°C. The pellet was resuspended in homogenization buffer, homogenized again in a dounce homogenizer on ice (20 times, 1,000 rpm). The homogenate was centrifuged at 800× *g* for 5 min at 4°C. The supernatant was collected, combined, and centrifuged at 8,000× *g* for 10 min at 4°C to pellet down the mitochondria. Mitochondria pellet was resuspended in homogenization buffer. Crosslinking was performed by adding 0.5 mM DSSO (Thermo Fisher Scientific, resuspended freshly in anhydrous DMSO to 50 mM), and incubated at room temperature for 20 min. 0.5 mM DSSO was added again and incubated for another 20 min. The reaction was quenched by adding 50 mM Tris, pH 8.0, at room temperature for 30 min. The crosslinked mitochondria were pelleted at 8,000× *g* for 10 min and stored at −20°C for further analysis.

Crosslinking and LC/MS analysis

The crosslinked samples were denatured with lysis buffer (8 M urea in 50 mM triethylammonium bicarbonate), reduced with 5 mM DTT at 56°C for 30 min, and alkylated with 40 mM 2-chloroacetamide for 30 min in the dark at room temperature. Crosslinked proteins are digested with Lys-C for 4 h at 37°C and subsequently digested by trypsin overnight. The resulting peptide mixture was desalted using Sep-Pak C18 cartridges (Waters), dried under vacuum, and fractionated by strong cation exchange (SCX) chromatography as previously described [32] to enrich higher charged crosslinked peptides. LC-MS experiments were performed using an ultra-HPLC Agilent 1200 System (Agilent Technologies), equipped with an in-house-packed C18 column for reversed-phase separation (column material: Poroshell 120 EC-C18, 2.7 μm (Agilent Technologies)), and coupled online to an Orbitrap Fusion mass spectrometer (Thermo Fisher Scientific). Mass analysis was performed using a previously described CID-MS2-MS3-ETD-MS2 acquisition method [32]. Data analysis was accomplished using XlinkX v2.0 software [32]. The following parameters were used, MS ion mass tolerance: 10 ppm; MS2 ion mass tolerance: 20 ppm; MS3 ion mass tolerance, 0.6 Da; fixed modification: Cys carbamidomethylation; variable modification: Met oxidation; enzymatic digestion: trypsin; and allowed number of missed cleavages: 3. All MS2 and MS3 spectra were searched against concatenated target-decoy databases generated based on the MitoCarta 2.0 database, containing 1,520 target sequence entries [33]. Crosslinks were identified at a 1% false discovery rate based on a target–decoy calculation strategy [32].

Statistical analysis

Data in graphs are represented as means ± SEM, and statistical significance of differences between groups was assessed by Student's *t*-test (unpaired or paired, one-tailed).

Image procession

Images were processed with Adobe Photoshop CS5.1.

Expanded View for this article is available online.

Author contributions

Author contributions: CW, RR-D, SD, and PR developed the concept of the study. CW, SD, RR-D, DP-G and YZ performed the experiments; CW, SD, and PR wrote the original draft. CW, SD, RR-D, FL, and PR reviewed and edited the final draft of the manuscript. SD and PR provided supervision.

Conflict of interest

The authors declare that they have no conflict of interest.

References

1. Chacinska A, Koehler CM, Milenkovic D, Lithgow T, Pfanner N (2009) Importing mitochondrial proteins: machineries and mechanisms. *Cell* 138: 628–644

2. Hällberg BM, Larsson N-G (2014) Making proteins in the powerhouse. *Cell Metab* 20: 226–240

3. Ott M, Herrmann JM (2010) Co-translational membrane insertion of mitochondrially encoded proteins. *Biochim Biophys Acta Mol Cell Res* 1803: 767–775

4. Richter-Dennerlein R, Dennerlein S, Rehling P (2015) Integrating mitochondrial translation into the cellular context. *Nat Rev Mol Cell Biol* 16: 586–592

5. Thompson K, Mai N, Oláhová M, Scialó F, Formosa LE, Stroud DA, Garrett M, Lax NZ, Robertson FM, Jou C *et al* (2018) OXA1L mutations cause mitochondrial encephalopathy and a combined oxidative phosphorylation defect. *EMBO Mol Med* 10: e9060

6. Hell K, Neupert W, Stuart RA (2001) Oxa1p acts as a general membrane insertion machinery for proteins encoded by mitochondrial DNA. *EMBO J* 20: 1281–1288

7. Signes A, Fernandez-Vizarra E (2018) Assembly of mammalian oxidative phosphorylation complexes I-V and supercomplexes. *Essays Biochem* 62: 255–270

8. Fernandez-Vizarra E, Tiranti V, Zeviani M (2009) Assembly of the oxidative phosphorylation system in humans: what we have learned by studying its defects. *Biochim Biophys Acta Mol Cell Res* 1793: 200–211

9. Timón-Gómez A, Nývltová E, Abriata LA, Vila AJ, Hosler J, Barrientos A (2018) Mitochondrial cytochrome c oxidase biogenesis: recent developments. *Semin Cell Dev Biol* 76: 163–178

10. Herrmann JM, Woellhaf MW, Bonnefoy N (2013) Control of protein synthesis in yeast mitochondria: the concept of translational activators. *BBA Mol Cell Res* 1833: 286–294

11. Ghezzi D, Zeviani M (2018) Human diseases associated with defects in assembly of OXPHOS complexes. *Essays Biochem* 62: 271–286

12. Shoubridge EA (2001) Nuclear genetic defects of oxidative phosphorylation. *Hum Mol Genet* 10: 2277–2284

13. Koopman WJH, Distelmaier F, Smeitink JAM, Willems PHGM (2013) OXPHOS mutations and neurodegeneration. *EMBO J* 32: 9–29

14. Shoubridge EA (2001) Cytochrome c oxidase deficiency. *Am J Med Genet* 106: 46–52

15. Giachin G, Bouverot R, Acajjaoui S, Pantalone S, Soler-López M (2016) Dynamics of human mitochondrial complex I assembly: implications for neurodegenerative diseases. *Front Mol Biosci* 3: 767

16. Stroud DA, Surgenor EE, Formosa LE, Reljic B, Frazier AE, Dibley MG, Osellame LD, Stait T, Beilharz TH, Thorburn DR *et al* (2016) Accessory subunits are integral for assembly and function of human mitochondrial complex I. *Nature* 538: 123–126

17. Guerrero-Castillo S, Baertling F, Kownatzki D, Wessels HJ, Arnold S, Brandt U, Nijtmans L (2017) The assembly pathway of mitochondrial respiratory chain complex I. *Cell Metab* 25: 128–139

18. Richter-Dennerlein R, Oeljeklaus S, Lorenzi I, Ronsör C, Bareth B, Schendzielorz AB, Wang C, Warscheid B, Rehling P, Dennerlein S (2016) Mitochondrial protein synthesis adapts to influx of nuclear-encoded protein. *Cell* 167: 471–483.e10

19. Mick DU, Dennerlein S, Wiese H, Reinhold R, Pacheu-Grau D, Lorenzi I, Sasarman F, Weraarpachai W, Shoubridge EA, Warscheid B *et al* (2012) MITRAC links mitochondrial protein translocation to respiratory-chain assembly and translational regulation. *Cell* 151: 1528–1541

20. Aich A, Wang C, Chowdhury A, Ronsör C, Pacheu-Grau D, Richter-Dennerlein R, Dennerlein S, Rehling P (2018) COX16 promotes COX2 metallation and assembly during respiratory complex IV biogenesis. *Elife* 7: 34

21. Ostergaard E, Weraarpachai W, Ravn K, Born AP, Jønson L, Duno M, Wibrand F, Shoubridge EA, Vissing J (2015) Mutations in COA3 cause isolated complex IV deficiency associated with neuropathy, exercise intolerance, obesity, and short stature. *J Med Genet* 52: 203–207

22. Weraarpachai W, Sasarman F, Nishimura T, Antonicka H, Auré K, Rötig A, Lombès A, Shoubridge EA (2012) Mutations in C12orf62, a factor that couples COX I synthesis with cytochrome c oxidase assembly, cause fatal neonatal lactic acidosis. *Am J Hum Genet* 90: 142–151

23. Zurita Rendon O, Shoubridge EA (2012) Early complex I assembly defects result in rapid turnover of the ND1 subunit. *Hum Mol Genet* 21: 3815–3824

24. Zurita Rendón O, Silva Neiva L, Sasarman F, Shoubridge EA (2014) The arginine methyltransferase NDUFAF7 is essential for complex I assembly and early vertebrate embryogenesis. *Hum Mol Genet* 23: 5159–5170

25. Zurita Rendón O, Antonicka H, Horvath R, Shoubridge EA (2016) A mutation in the flavin adenine dinucleotide-dependent oxidoreductase FOXRED1 results in cell-type-specific assembly defects in oxidative phosphorylation complexes I and II. *Mol Cell Biol* 36: 2132–2140

26. Dunning CJR, McKenzie M, Sugiana C, Lazarou M, Silke J, Connelly A, Fletcher JM, Kirby DM, Thorburn DR, Ryan MT (2007) Human CIA30 is involved in the early assembly of mitochondrial complex I and mutations in its gene cause disease. *EMBO J* 26: 3227–3237

27. Nouws J, Nijtmans L, Houten SM, van den Brand M, Huynen M, Venselaar H, Hoefs S, Gloerich J, Kronick J, Hutchin T *et al* (2010) Acyl-CoA dehydrogenase 9 is required for the biogenesis of oxidative phosphorylation complex I. *Cell Metab* 12: 283–294

28. Ran FA, Hsu PD, Wright J, Agarwala V, Scott DA, Zhang F (2013) Genome engineering using the CRISPR-Cas9 system. *Nat Protoc* 8: 2281–2308

29. Hsu PD, Scott DA, Weinstein JA, Ran FA, Konermann S, Agarwala V, Li Y, Fine EJ, Wu X, Shalem O *et al* (2013) DNA targeting specificity of RNA-guided Cas9 nucleases. *Nat Biotechnol* 31: 827–832

30. Wittig I, Braun H-P, Schägger H (2006) Blue native PAGE. *Nat Protoc* 1: 418–428

31. Faloona GR, Srere PA (1969) Escherichia coli citrate synthase. Purification and the effect of potassium on some properties. *Biochemistry* 8: 4497–4503

32. Liu F, Lössl P, Scheltema R, Viner R, Heck AJR (2017) Optimized fragmentation schemes and data analysis strategies for proteome-wide cross-link identification. *Nat Commun* 8: 15473

33. Calvo SE, Clauser KR, Mootha VK (2016) MitoCarta2.0: an updated inventory of mammalian mitochondrial proteins. *Nucleic Acids Res* 44: D1251–D1257